Mechanisms of Crack Closure in Plane Strain and in Plane Stress

Huseyin Sehitoglu, Wei Sun
Department of Mechanical and Industrial Engineering
University of Illinois, Urbana, Ill.61801

Third International Conference on Biaxial/Multiaxial Fatigue
April 3-6, 1989 Stuttgart, FRG

Abstract

The purpose of this paper is to study the inelastic stress-strain fields in the proximity of fatigue cracks under plane stress and plane strain conditions. An elastic-plastic finite element solution using linear kinematic hardening that permits crack growth through the mesh is used. Results provide insight into closure behavior as influenced by different constraint cases (plane stress versus plane strain). The results unveil inelastic strain accumulation in the y-direction (applied load direction) ahead of crack tip under both plane stress and plane strain conditions. While material transfer to crack flanks from progressive contraction in z-direction (thickness direction) is known to contribute to crack closure in plane stress, the mechanism of crack closure in plane strain is less understood. Strain accumulation in the x-direction (along the crack growth direction) causing progressive contraction of material ahead of crack tip is found in plane strain. Upon crack advance this in turn contributes to transfer of material to crack flanks and the development of closure in plane strain.

Nomenclature

a	Crack Length
B	Specimen Thickness
d	Contact Distance Behind Crack Tip
$d\bar{\varepsilon}^p$	Equivalent Plastic Strain Increment
$d\varepsilon_{ij}^p$	Plastic Strain Rate Tensor
dS_{ij}^c	Deviatoric Back Stress Tensor
E	Modulus of Elasticity
H	Plastic Modulus ($d\bar{\sigma}/d\bar{\varepsilon}^p$)
K_{max}	Maximum Stress Intensity
n	Step Number
P_{max}	Maximum Applied Load Level
P_{open}	Applied Load Level at Crack Opening

P_o	Reference Load
r	Distance Behind the Crack Tip
r_p	Reversed Plastic Zone Size (Active Plastic Zone at Minimum Load)
R	Stress Ratio
s_{ij}, s^c_{ij}	Deviatoric Stress,Deviatoric Back Stress Tensor
x,y,z	Coordinate Axis
W	Specimen Width
$\alpha_x,\alpha_y,\alpha_z$	Normal Back Stress Components
δ	Crack Opening Displacement
ε^p_x ,ε^p_y,ε^p_z	Normal Plastic (Inelastic) Strain Components
ε_x ,ε_y,ε_z	Normal Strain Components
σ_o	Yield Strength
$\bar{\sigma}$	Von Mises Equivalent Stress

1.Introduction

It is well known that crack closure has a first order influence on fatigue crack growth rates. Crack closure phenomena was discovered by Elber in early 1970's and his measurements of surface displacements provided insight into closure behavior under plane stress conditions [1]. Later research involving bulk measurements such as compliance, back face strain gage, potential drop and other methods showed that closure occurred under plane strain conditions [2].

Analytical and numerical methods of crack closure prediction evolved over the years [2-10]. The analytical models are primarily based on the Dugdale strip yield model and hold for plane stress conditions. In plane stress, contraction in the thickness direction provides the material transferred to crack surfaces. This material represents the residual displacements. Therefore, during cycling a crack may close before the minimum load is reached. Dugdale type closure models [3, 8-9] provided valuable insight into dependence of closure load on R-ratio, applied load level and crack size. However, Dugdale models of crack closure are not capable of accounting for material hardening, Bauschinger effect, complex loading directions and geometry effects, furthermore numerous assumptions are adopted on residual displacements, residual stress distributions and uniaxiality of stresses.

A diffuse plastic zone with maximum shear planes intersecting the specimen surfaces at 45 degrees is inherent in the Dugdale model. Orientations of the planes of maximum shear are different in plane strain, therefore Dugdale model does not apply to plane strain conditions. Plane strain closure levels need to be determined by finite element analysis. Despite the significance of plane strain, only limited finite element analyses have been conducted [4, 5, 8, 10]. The mechanisms that

contribute to crack closure in plane strain have not been identified. Furthermore, the inelastic deformation fields in plane strain versus plane stress under fatigue crack growth conditions have not been described.

In plane strain, the mechanism of material transfer to crack surfaces from thickness contraction is not operative, however material transfer in x-direction (along the crack growth direction) provides residual displacements contributing to crack closure.

The purpose of this paper is to describe the mechanisms of material transfer to crack surfaces in plane strain and plane stress and elucidate the process of crack closure. Inelastic strain accumulations in x and z directions have been identified to confirm these mechanisms of material transfer in plane strain and plane stress respectively.

The results are presented for R=0 loading conditions in a compact tension geometry. They indicate that crack opening and closure load levels are lower in plane strain compared to plane stress. This is found consistent with higher constraint on material transfer in plane strain compared to plane stress.

2.Geometry and Material Model

Crack opening and crack closure behavior of cracks growing in compact tension specimen in plane strain and plane stress conditions is studied with a finite element analysis. The finite element mesh used in this study is shown in Figure 1a. The specimen width, W, is 2 inches and crack size, a, of 1.2 inches was considered. Due to symmetry only one half of the CT geometry is modelled. The x-y directions are indicated in the diagram, the z-direction is the thickness direction. A magnified view of near crack tip is shown in Figure 1b. The size of quadrilateral elements at the crack tip is as small as 0.0015 inches. This size is fine enough to capture forward and reversed plastic zone at the crack tip for the cases considered. Spring elements are attached to the elements along the x-axis to simulate opening and closure of the fatigue crack. The crack is advanced

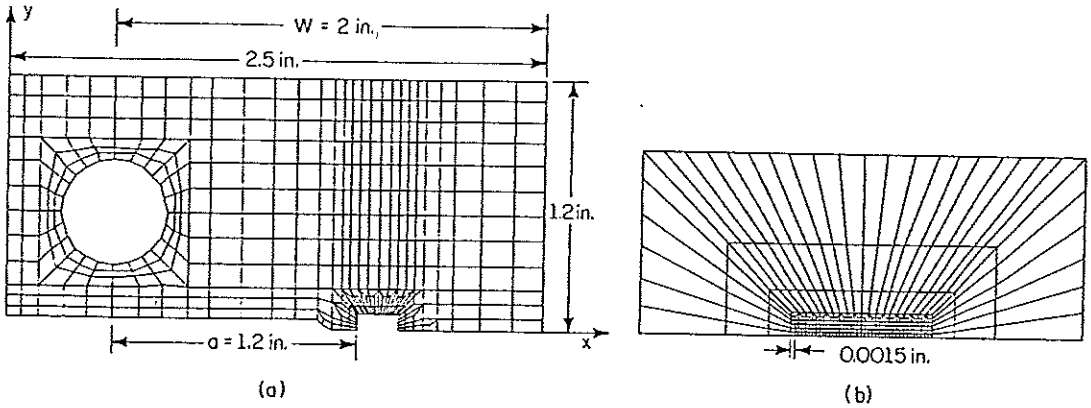

Figure 1 F.E.M mesh showing the compact tension specimen and the fine mesh near the crack tip.

every cycle over approximately 20 cycles and crack opening and crack closure load levels were determined. The crack opening load levels increase with cycles and may reach near stabilized levels.

The results are presented for a/W=0.6 (a=1.2 inches) conditions. Simulations for a/W=0.3 case were also conducted and the results were similar to the a/W=0.6 case. Note that for the a/W=0.3 case extensive yielding at the hole (where remote loading is applied) is encountered. In the a/W=0.6 case the applied load levels were lower, therefore yielding near the hole did not occur. The applied load levels are given as P_{max}/P_o ratio where P_o is the calculated reference load and is given as $1.455\beta(W-a)B\sigma_o$ for plane strain and as $1.071\beta(W-a)B\sigma_o$ for plane stress, where β=0.122 for a/W=0.6, B=1 inch, σ_o= 63 ksi, W=2 inches and a=1.2 inches. Crack opening and closure levels for P_{max}/P_o ratios in the range 0.1 to 1 are reported in this study. Specifically, P_{max}/P_o=0.2 and 0.5 cases will be discussed in depth. The corresponding maximum stress intensity levels were 13 ksi$\sqrt{in}$ (0.2) and 32 ksi$\sqrt{in}$ (0.5) for plane stress case, 17 ksi$\sqrt{in}$ (0.2) and 43 ksi$\sqrt{in}$ (0.5) for plane strain case.

The simulations were conducted for R=0 and R=-1 conditions. Only R=0 results will be discussed in this study, however conclusions hold for R=-1 cases also. It is noted that there are some basic differences between the CT specimen conditions examined here and the centered crack tension (CCT) specimens examined in early work [4-7]. With the CT specimen the ratio of reversed plastic zone size with respect to crack size, or with respect to specimen width is smaller compared to CCT specimen for a given P_{max}/P_o ratio. Furthermore, the initial (sawcut) crack size in CT specimen over which residual displacements can not exist occupy a large portion of total crack size. In certain cases this would result in lower crack opening loads compared to the cracks with the full plastic wake.

The constitutive model is based on Von Mises yield surface translating according to Ziegler's rule. The hardening modulus /elastic modulus ratios (H/E) of 0.01 and 0.07 have been studied. The σ_o/E ratio considered was 0.002 where E is the elastic modulus (30,000 ksi or =2.05 x 10^5 MPa). To avoid mesh locking in plane strain, Nagtegaal, Parks and Rice [11] reduced integration modification has been incorporated in the formulation. The inelastic strain rate is related to the stress in the following form

$$d\varepsilon_{ij}^{p} = \frac{3}{2}\frac{d\bar{\varepsilon}^{p}}{\sigma_o}(S_{ij} - S_{ij}^{c}) \qquad (1)$$

where $d\bar{\varepsilon}^{p}$ is equivalent plastic strain increment, S_{ij} is the deviatoric stress tensor and S_{ij}^{c} is the deviatoric back stress tensor. The evolution of back stress is given in Ziegler's form as

$$dS_{ij}^{c} = d\mu\,(S_{ij} - S_{ij}^{c}) \qquad (2)$$

where $d\mu$ is the scalar determined from the consistency condition. Note that $d\varepsilon_{ii}^{p} = 0$ hence incompressibility is satisfied. The results have been checked against ABAQUS Finite Element Code for the stationary crack cases and the stresses and strains between our code and ABAQUS agree within 2%. The finite element simulations were conducted using a CRAY-XMP48 supercomputer located in National Center for Supercomputer Applications at University of Illinois. Typical execution times were of the order of 0.5 hour per simulation.

3. Mechanisms of Crack Closure in Plane Strain versus Plane Stress

Before considering the results of simulations, it is instructive to outline the mechanisms of material transfer to crack surfaces as the crack advances. Consider Figure 2a where an angled view of the crack plane is depicted. The x-y-z directions are indicated as well as the r direction defined as a-x and the location of crack front. In the case of plane stress, contraction in z-direction develops and the material at crack front (dashed region) is transferred into crack flanks. The material transfer directions are indicated with arrows. The distance r_p is the projected reversed plastic zone size, this is the active plastic zone at minimum load of the cycle.

In the case of plane strain, the contraction in z-direction is zero, or total strain in z-direction is zero. This material does not contribute to crack closure. However, an alternate mechanism involving contraction of material in x-direction at crack front provides material that would enter crack surfaces and cause crack closure. The dashed region in Figure 2b depicts this material and the arrows indicate the motion of material upon crack advance.

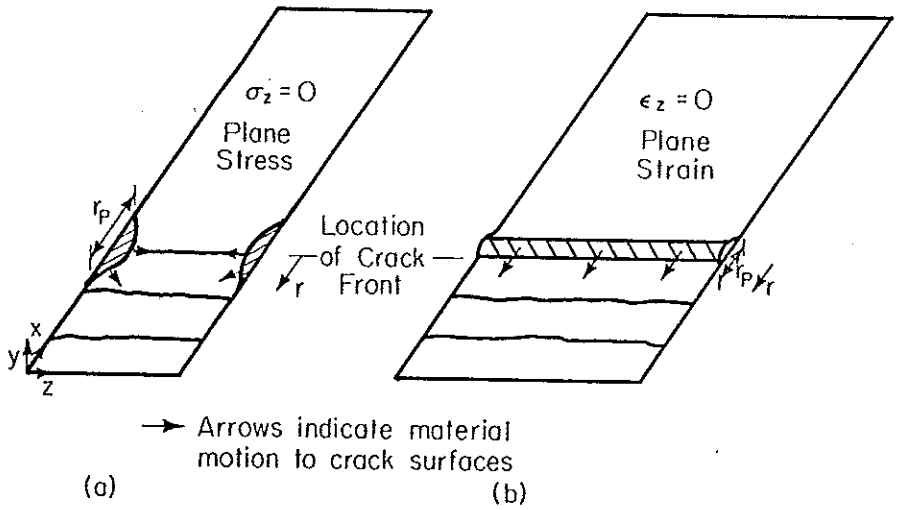

Figure 2a Crack planes indicating mechanism of material transfer in plane stress (schematic)

Figure 2b Crack planes indicating mechanism of material transfer in plane strain (schematic)

The crack opening displacements corresponding to maximum load and minimum load are indicated in Figure 2c. The residual displacements arising from contraction in z-direction and contraction in x-direction are indicated. Note that closure due to x-contraction is operative primarily in plane strain but it does exist to a lesser extent in plane stress. These residual material cause premature contact of crack surfaces before the minimum load in the cycle is reached. The load at which first contact of crack surfaces occur is defined as the crack closure load. Once the crack surfaces contact compressive stresses develop. In Figure 2c compressive stresses would exist over the region 0<r<d. Upon loading, the compressive stresses need to be overcome before the crack surfaces can open .The load at which residual compressive stresses are overcome is defined as crack opening load, P_{open}.

The plane stress and plane strain conditions described represent conditions operating at the surface and in the interior of a cracked body respectively. Therefore, material transfer to crack flanks at the specimen surface and in the interior would be different. Bulk closure measurements would represent a combination of plane stress and plane strain cases, with plane strain conditions dominating when the r_p with respect to specimen thickness is small.

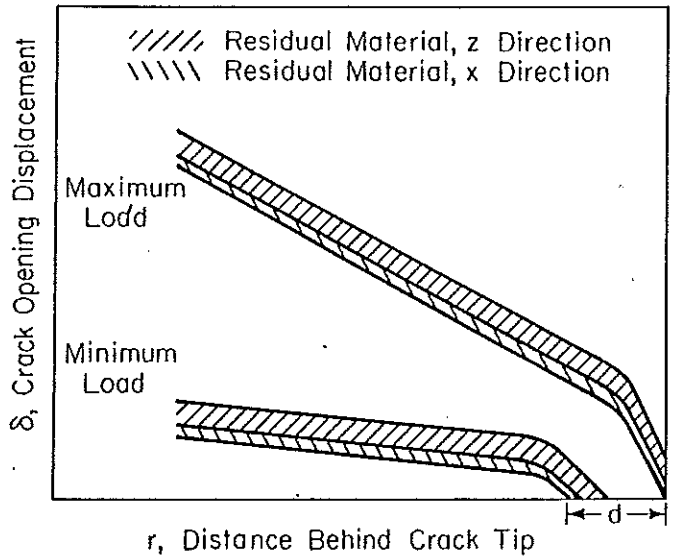

Figure 2c Crack opening displacements at maximum load and at minimum load indicating residual material on crack surfaces due to material transfer from z and x directions

4. Stress-strain Fields in Plane Strain

To understand the factors causing crack closure in plane strain, the strain fields including inelastic strain fields in the vicinity of a fatigue crack as crack advances are studied.

4.1. P_{max}/P_o=0.2 Case

The case P_{max}/P_o=0.2 is considered first. The change in load with step number is indicated in Figure 3a where n refers to step number. To reach maximum load in the cycle 20 steps are taken, and 20 steps are required during unloading to zero load. Therefore at the conclusion of 20 cycles 800 steps are utilized. The crack is advanced every cycle during the first increment of unloading (Step #21, 61, 101, 141, etc.). The elements including the spring elements along the crack path and nodes are indicated in Figure 3b. Initially, the crack tip is at Node #295.

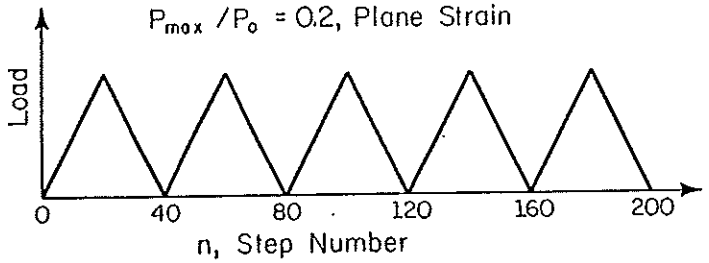

Figure 3a The load variation with Step Number for the case P_{max}/P_o=0.2.

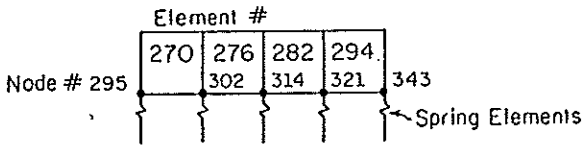

Figure 3b The elements along the crack path. Element #282 lower left integration point is defined as the "material point".

The stress-strain behavior in y and x directions over the first 160 steps at lower left integration point of Element #282 as the crack advances is indicated in Figures 4-5. The vertical axis is stress normalized by yield strength. The lower left integration point in Element #282 is referred to as "material point". Element #282 is the third element away from the original location of the crack.tip Crack tip reaches this element in three cycles. At Step #20 the material point is three elements distant from the crack tip which is at node point #295. Therefore in the first cycle the inelastic strains are less than 0.001. Upon subsequent cycling, gradual accumulation of inelastic strains in positive y and negative x directions develop simultaneously as the crack approaches the "material point". At Step #100, Node #314 is the crack tip and "material point "is reached, the stress levels in x and y directions reach their maximum. At Step #140 the crack tip has passed the "material point" and the stresses at the material point are lowered.

The series of crack opening and closure events are summarized in Table 1 where the status of each node is given at different step numbers. Note that the crack tip opens at Step #126 therefore the P_{open}/P_{max} ratio is 0.33 after three cycles. Upon unloading the location of the crack tip

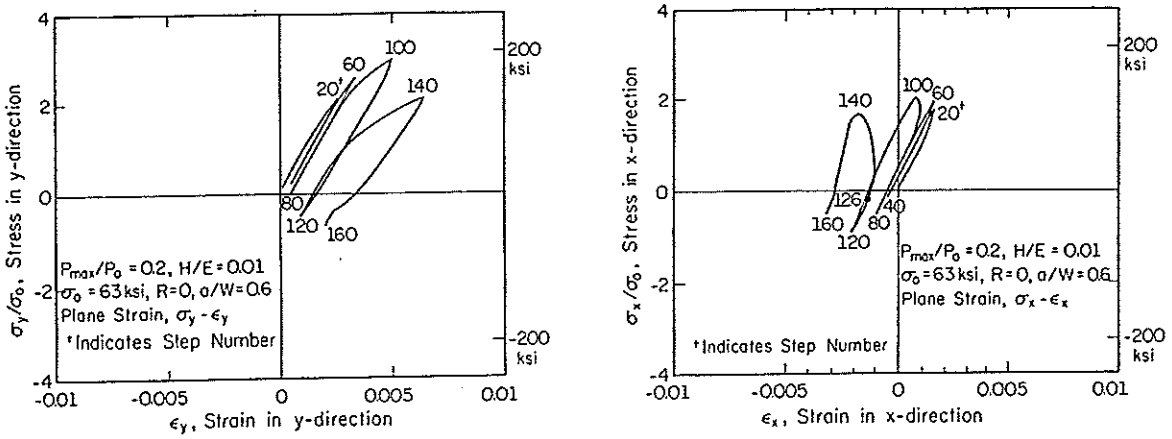

Figure 4 Stress-strain (y-direction) at 'material point' from Step #1 through 140. At Step #100 the crack tip has reached Element #282 (P_{max}/P_o=0.2. plane strain Case).

Figure 5 Stress-strain (x-direction) at 'material point' from Step #1 through 140. At Step #100 the crack tip has reached Element #282 (P_{max}/P_o=0.2 plane strain Case).

Table 1 Series of crack opening and closure events for P_{max}/P_o=0.2 case

Step #	Status
86	Node #302 open, Node #314 becomes the crack tip
101	Node #314 released, but closes immediately
117	Node #302 closed, Node #302 becomes the crack tip
124	Node #302 open, Node #314 becomes the crack tip
126	Node #314 open, crack tip passes Element #282
157	Node #302 closed, Node #314 still open, discontinous crack closure
158	Node #314 closed ,crack tip is at Node #302

Table 2 Summary of stresses,strains, back stresses at maximum and minimum load as the crack approaches, reaches and passes the "material point".(P_{max}/P_o=0.2 case)

Pmax/Po=0.2 , H/E=0.01, σ_o =63 ksi
R=0 , a/W=0.6 , Plane Strain

	Max. Load	Min. Load	Max. Load	Min. Load	Max. Load	Min. Load
Step #	60	80	100	120	140	160
σ_x	109+	-26	111	-57	91	-24
ϵ_x	0.0013	-0.0009	0.0002	-0.0022	-0.0020	-0.0031
ϵ_x^p	0	0	-0.0006	-0.0006	-0.0029	0.0029
α_x	0.06	0.06	0.8	0.8	4.3	4.6
σ_y	150	7	174	-32	116	-45
ϵ_y	0.0032	0.0006	0.0051	0.0010	0.0061	0.0020
ϵ_y^p	0.0001	0.0001	0.0015	0.0015	0.0041	0.0031
α_y	0.08	0.08	1.2	1.2	6.5	6.3
σ_z	80	-3	112	1	99	-11
ϵ_z	0	0	0	0	0	0
ϵ_z^p	-0.0001	-0.0001	-0.0009	-0.0009	-0.0012	-0.0003
α_z	0.04	0.04	0.7	0.7	5	5.5

\+ Stresses and back stresses are given in ksi

changes and for example at Step #158 the crack tip returns to Node #302. Note that discontinous crack closure has occurred during the fourth cycle where at Step #157 Node #314 is still open while Node #302 is closed.

The stresses including the back stresses, strains including inelastic strains at maximum and minimum load levels are summarized in Table 2. Note that the incompressibility condition is satisfied for the plastic strain components such that the summation of plastic strain components is zero. Note that $\alpha_x, \alpha_y, \alpha_z$ refer to back stress components. Due to the low hardening modulus (H/E=0.01) the back stresses are a small fraction of the stress components. Note that the "material point" also undergoes shear stress and shear strain but these are not included in the Table for simplicity.

The stress-strain response for the first four cycles is discussed above. If hysteresis loops after 10 or more cycles are shown the results would be qualitatively similar. However, note that the crack opening load is not stabilized after three cycles and the crack opening loads increase to their steady state levels with increasing number of cycles.

4.2 P_{max}/P_o=0.5 Case

The change in load with step number is indicated in Figure 6 for the P_{max}/P_o=0.5 case. The step number to reach maximum load is increased to 40 in this case. This improves the resolution in determining the crack opening load level. The material point considered is again the lower left integration point of Element #282. The stress-strain behavior for this case is illustrated in Figures 7-8 and the crack opening and closure information is given in Table 3. In the case of P_{max}/P_o=0.5 the crack tip inelastic strains are higher and significant mean stress decrease with cycles is observed compared to P_{max}/P_o=0.2 case.

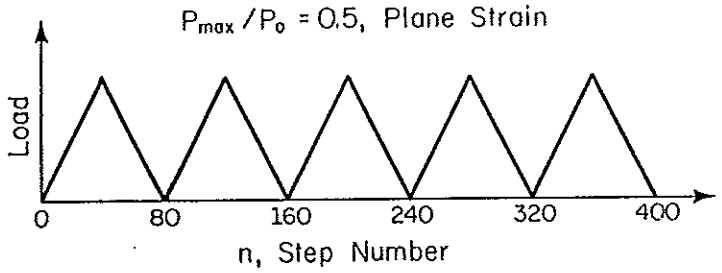

Figure 6 The Load variation with Step Number for the case P_{max}/P_o=0.5

Note that in this case there is a stronger previous history effect on the strains at crack tip as the material point is approached. Strain accumulation approaching 0.02 has been observed both in x and y directions. The tensile stresses at the material point decrease as the crack tip approaches it. If the material point is reached in higher number of cycles the mean stress relaxation would be more significant. Once the crack

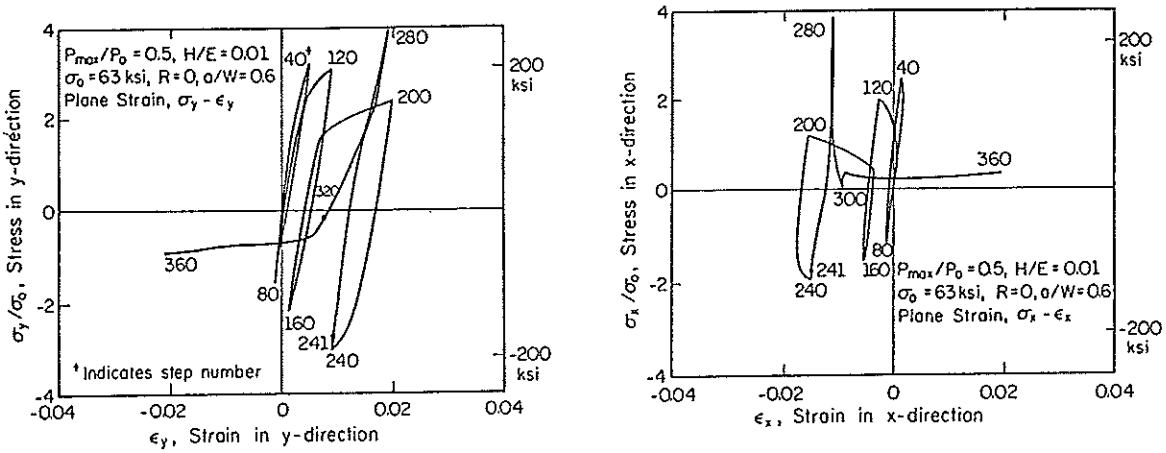

Figure 7 Stress-strain (y-direction) at 'material point' from Step #1 through 360. At Step #200 the crack tip has reached Element #282.

Figure 8 Stress-strain (x-direction) at 'material point' from Step #1 through 360. At Step #200 the crack tip has reached Element #282.

Table 3 Series of crack opening and closure events for P_{max}/P_o=0.5 case

Step #	Status
162	Node #302 open, Node #314 becomes the crack tip
201	Node #314 released, but closes immediately
241	Node #314 open, crack tip passes Element #282

tip passes the material point, the stresses increase as indicated in Figures 7 and 8. This appears contradictory to early results, however it has been repeatedly observed for P_{max}/P_o ratios above 0.4. The Element #282 at Step #280 in this case remains on the vertices of the blunted crack profile where high stresses and triaxiality of stress prevail. Summary of stresses, strains, back stresses at maximum load and at minimum load as crack approaches the material point, reaches the material point and passes the material point are indicated in Table 4.

Table 4 Summary of stresses,strains, back stresses at maximum and minimum load as the crack approaches, reaches and passes the "material point".(P_{max}/P_o=0.5 case)

Pmax/Po=0.5 , H/E=0.01, σ_o =63 ksi
R=0 , a/W=0.6 , Plane Strain

	Max. Load	Min. Load	Max. Load	Min. Load	Max. Load	Min. Load
Step #	120	160	200	240	280	320
σ_x	124	-100	74	-124	239	2
ϵ_x	-0.0026	-0.0054	-0.0155	-0.0149	-0.0108	-0.0093
ϵ_x^p	-0.0032	-0.0041	-0.0153	-0.0141	-0.0139	-0.0095
α_x	3.1	2.5	6.1	3.2	59	60
σ_y	197	136	152	-189	250	-7
ϵ_y	0.0089	0.0014	0.0200	0.0088	0.0193	0.0078
ϵ_y^p	0.0051	0.0043	0.0168	0.0125	0.0157	0.0080
α_y	4.7	4.1	12.4	8.4	67	63
σ_z	153	-65	113	-143	242	-1
ϵ_z	0	0	0	0	0	0
ϵ_z^p	-0.0019	-0.0002	-0.0015	0.0017	-0.0032	0.0007
α_z	3.3	3.3	8.9	6.4	61	61

The crack opening displacements at maximum load at Step #200 and at minimum load at Step #240 are given in Figure 9a. Crack opening displacements over the region of the crack with no wake are included in this figure (r extends from 0 to 0.18 inches). Note that in this case the crack tip opens in the second increment of loading (Step #162, P_{open}/P_{max}=0.05) and the steady state crack opening load level is P_{open}/P_{max}=0.1. The crack contact zone is limited to one element behind the crack tip. The region near the crack tip is shown in Fig 9b. Note that in this figure r extends from 0 to 0.0045 inches.

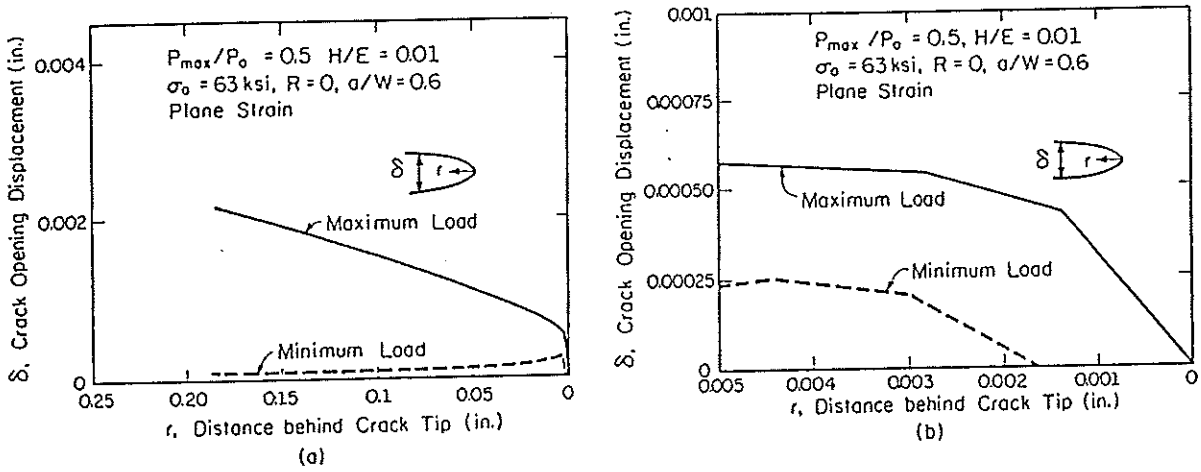

Figure 9a Crack opening displacements at maximum and minimum loads corresponding to P_{max}/P_o=0.5 plane strain case.

Figure 9b Crack opening displacements very near crack tip for P_{max}/P_o=0.5 plane strain case.

5. Stress-strain Fields in Plane Stress

The strain accumulation in x direction observed in plane strain case is not observed in plane stress. The stress-strain behavior at Element #282 is indicated in Figures 10 and 11 for y and x directions respectively. The stresses are normalized with respect to yield strength. The results correspond to P_{max}/P_o=0.2. Note that the stresses near the crack tip are lower compared to plane strain, however the accumulated strains are higher. The step numbers are indicated on the Figures. Once the crack tip passes the material point the tensile stress decreases in this case. The crack opening load level in this case is significantly higher than the plane strain case. The P_{open}/P_{max} ratio is 0.6.

Qualitatively similar results to P_{max}/P_o=0.2 is obtained for the P_{max}/P_o=0.5 plane stress case. The stress-strain behavior corresponding to P_{max}/P_o=0.5 is depicted in Figures 12 and 13. The crack opening displacement profiles at maximum load and at minimum load are indicated in Figure 14a. A detailed picture of the crack tip region is indicated in Figure 14b. Note that the region of contact of crack surfaces extends three elements behind the crack tip and crack closure is continous behind the crack tip .The crack opening load level in this case increases with cycles

and approaches P_{open}/P_{max}=0.45. The crack opening displacements for stationary cracks(cracks with no wake and no residual displacements) are given in Figure 15. These can be directly compared to growing crack results given as Figures 9 and 14.

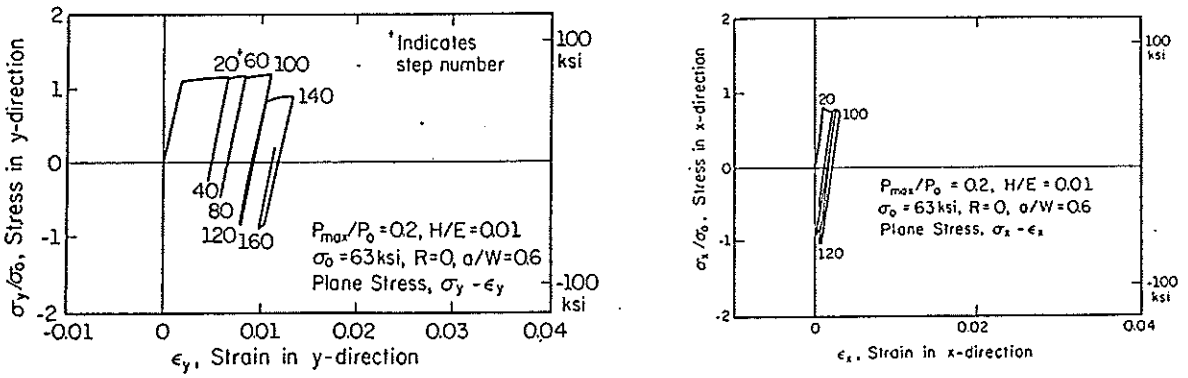

Figure 10 Stress-strain (y-direction) at 'material point' from Step #1 through 140. At Step #100 the crack tip has reached Element #282 (P_{max}/P_o=0.2 Plane Stress Case).

Figure 11 Stress-strain (x-direction) at 'material point' from Step #1 through 140. At Step #100 the crack tip has reached Element#282(P_{max}/P_o=0.2 Plane Stress Case).

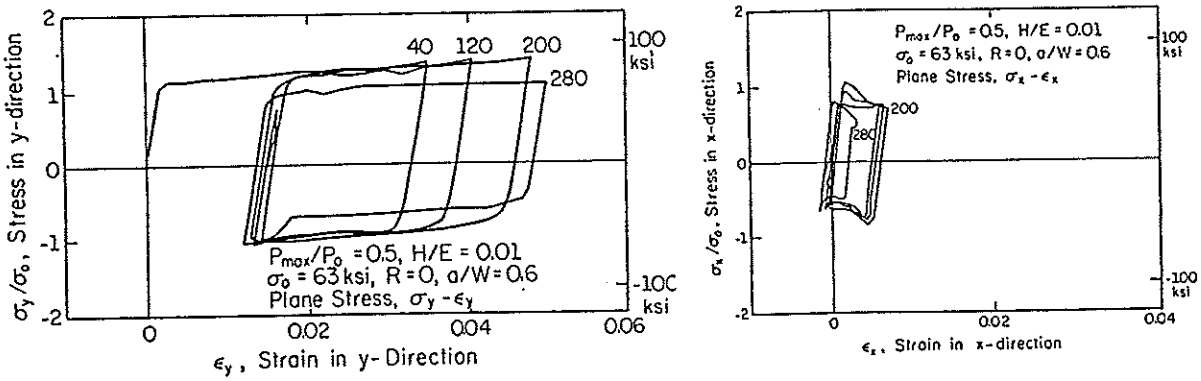

Figure 12 Stress-strain (y-direction) at 'material point' from Step#1 through 280 At Step #200 the crack tip has reached Element #282(P_{max}/P_o=0.5 Plane Stress Case).

Figure 13 Stress-strain (x-direction) at 'material point' from Step#1 through 280. At Step #200 the crack tip has reached Element#282(P_{max}/P_o=0.5 Plane Stress Case).

The normalized crack opening load levels for plane stress and plane strain cases are given in Figure 16. The P_{max}/P_o ratios in the range 0.2 to 1 are reported in this figure.

6. Discussion of Results

Results demonstrated that accumulation of strains in the x, y directions in plane strain and y, z directions in plane stress develop under

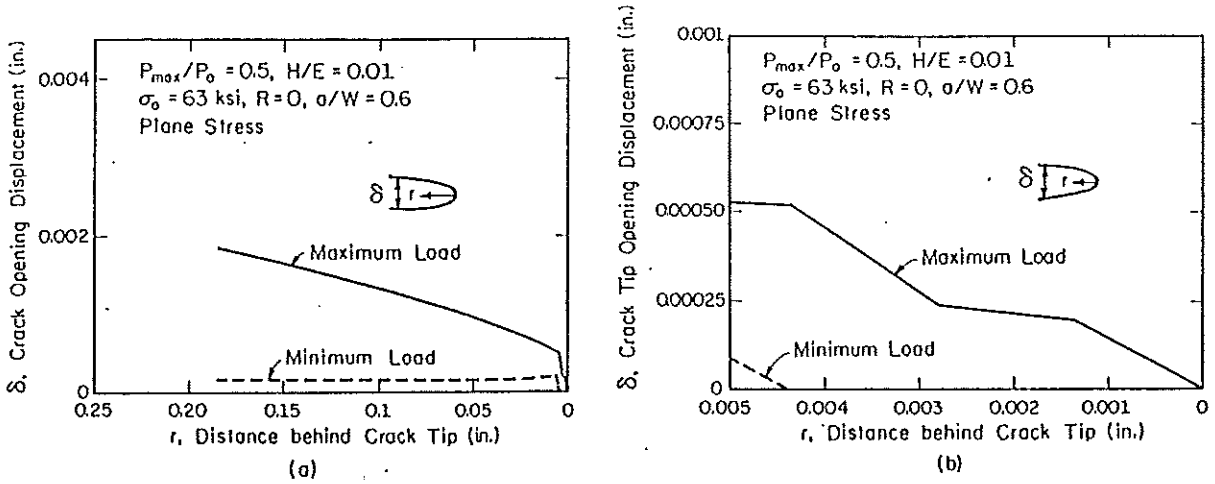

Figure 14a Crack opening displacements at maximum and minimum load for P_{max}/P_o=0.5 plane stress case.
Figure 14b Crack opening displacements very near crack tip for P_{max}/P_o=0.5 plane stress case.

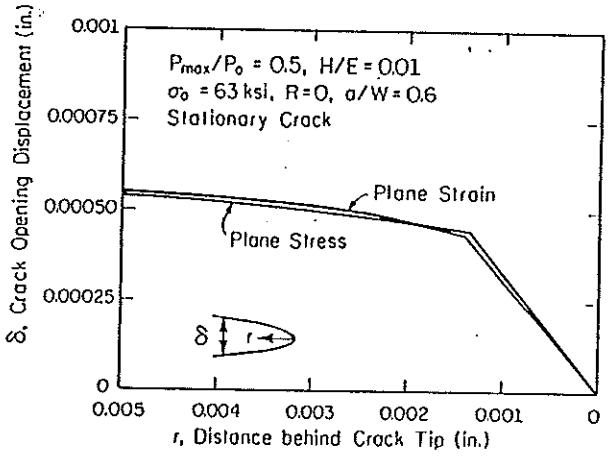

Figure 15 Crack opening displacements for stationary crack(with no wake) at maximum load for P_{max}/P_o=0.5 case.

cyclic loading. These influence the closure behavior in fatigue crack growth. Material transferred to crack flanks comes from thickness contraction in plane stress and transverse contraction in plane strain. The region over which the contraction in x-direction develops in plane strain extends over the reversed plastic zone. The material within the reversed plastic zone undergoes reversed plasticity with ratcheting. Similarly, in plane stress the contraction in z-direction occurs over the reversed plastic zone of the crack.

The results in Figure 16 indicate that crack opening load level is dependent on the maximum load with respect to reference load and the inelastic strain fields at crack tip. Note that at low maximum load levels such as P_{max}/P_o=0.2, the reversed plastic zone size is a small fraction of crack size (r_p/a=0.003 or r_p=0.0036 inches) and the strain accumulation is confined to crack tip. In the case of P_{max}/P_o=0.5 the reversed plastic zone is larger (r_p/a=0.025 or r_p=0.03 inches), the strain accumulation occurs

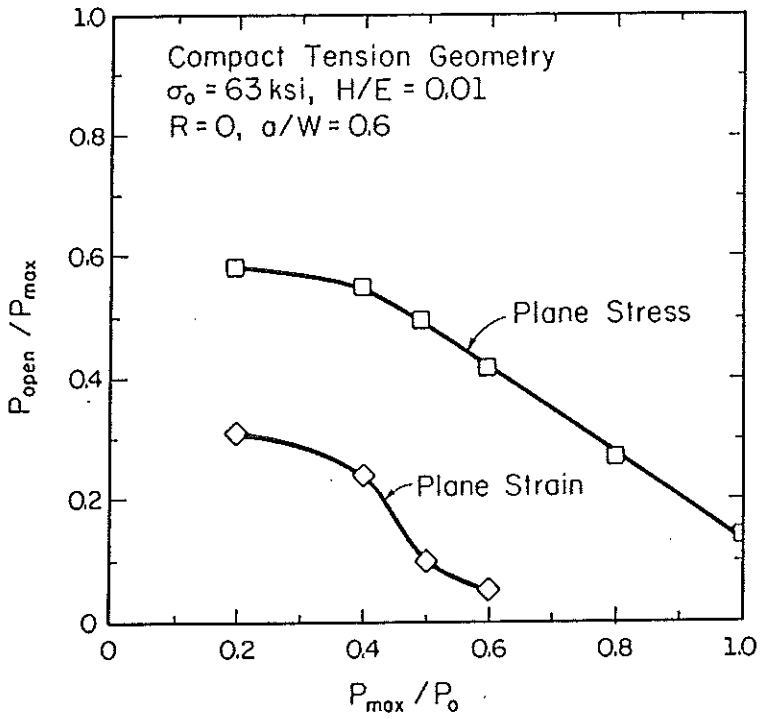

Figure 16 Summary of steady state crack opening load levels as a function of applied load for plane stress and plane strain cases for the CT geometry.

over a wider region. The strain accumulation influences the crack opening displacements including the residual displacements and the transient crack opening load levels. If the prior history effect is significant, the number of cycles to approach stabilized levels of crack closure could be larger than 20 cycles. The number of cycles required for opening load levels to saturate increases with increasing P_{max}/P_o ratio. This is consistent with results reported in this study and with early work by the authors [5,7].

It is noted that crack opening load levels in plane strain and plane stress decrease rapidly to zero for this geometry with increasing load levels. Similar trends hold for the CCT specimen. However the crack opening load levels are lower for the CT case. This may be readily attributed to the lack of residual displacements over the majority of the crack in the CT case. The crack opening load levels decreased also for the CCT geometry when a crack with a partial wake was considered (See Figure 15, Reference [5]).

Results are qualitatively similar if H/E ratio of 0.07 was considered. In this case considerable hardening is allowed and the back stress (hence the mean stress) levels in the cycles are higher. In the case of plane strain, the use of H/E =0.07 for P_{max}/P_o larger than 0.4 results in stress levels at crack tip that far exceed the fracture stress of engineering materials.

The results demonstrate that remote measurement techniques of crack closure such as clip gages, back face strain gages would have limitations in determination of crack opening and crack closure loads. The zone of material transfer and the contact zone is a very small fraction of the total crack size particularly for plane strain cases. Only direct

measurement of crack tip displacements would capture the true crack opening and closure load levels.

If a failure criteria is to be developed the history of deformation rather than the current stress (or strain) at a critical element must be considered. Attempts to use strain range or stress range at the crack tip alone as a failure criteria is not sufficient since mean stress and mean (accumulated) strain would have a significant influence. The results illustrate the complexity of these multiaxial stress-strain fields and demonstrate the limitations of uniaxial models of crack closure.

It is noted that only other work reported on finite element analysis of CT specimen is that of Blom and Holm [10], who reported P_{open}/P_{max}=0.3 for plane strain and and P_{open}/P_{max}=0.45 for plane stress case. Their P_{max}/P_0 ratio was 0.43 for plane strain and 0.2 for plane stress case. These results are in qualitative agreement with results reported in this study. Stress-strain behavior near crack tip is not available in their study therefore a direct comparison of results can not be made at this time.

7. Conclusions

1. In plane strain, mechanism of material transfer to crack surfaces through transverse (x-direction) contraction of material at crack tip is proposed. Inelastic strain accumulation in x-direction confirms the presence of this mechanism.

2. In plane stress, crack closure occurs due to a mechanism of material transfer to crack surfaces through thickness (z-direction) contraction.

3. Crack opening load levels for the compact tension specimen for plane strain and plane stress cases have been determined for R=0 loading. The normalized crack opening levels decrease with increasing maximum load level in both plane stress and plane strain cases and plane strain closure levels are lower.

4. Understanding of stress-strain history near crack tip is relevant to understanding crack growth mechanisms, and to determination of crack closure behavior. The results demonstrate these stress and strain fields are multiaxial .

8. Acknowledgements

The work is supported by the Fracture Control Program, University of Illinois. Computer access was gained with grants from the National Center for Supercomputer Applications, NCSA, University of Illinois. Discussions with Dr .Craig McClung, Southwest Research Institute, formerly graduate

student at University of Illinois are acknowledged.

9. References

1. Elber, W. "Fatigue Crack Propagation; Some Effects of Crack Closure on the Mechanism of Fatigue Crack Propagation under Cyclic Tension Loading" PhD Thesis ,University of New South Wales,Australia,1968.

2. ASTM STP 982, Mechanics of Fatigue Crack Closure, Newman/Elber Editors,1988

3. Budiansky, B.,J.Hutchinson, "Analysis of Closure in Fatigue Crack Growth", J. Applied Mechanics, V.45, 1978, pp.267-276.

4. Newman, J.C., "A Finite Element Analysis of Fatigue Crack Closure", ASTM STP 590, 1976, pp281-301.

5. Lalor, P., H.Sehitoglu, "Fatigue Crack Closure Outside the Small Scale Yielding Regime", ASTM STP 982, 1988, pp.342-360

6. Lalor, P., H.Sehitoglu, R.C.McClung," Mechanics Aspects of Small Crack Growth from Notches-The Role Crack Closure', The Behavior of Short Fatigue Cracks, EGF 1, Mechanical Engineering Publications, London, 1986, pp369-386.

7. McClung, R.C., H.Sehitoglu, "On The Finite Element Analysis of Crack Closure, Part One: Basic Modelling Issues; Part Two: Numerical Results", To appear in Engineering Fracture Mechanics

8. Sehitoglu, H., "Characterization of Crack Closure", ASTM STP 868, 1985, pp.361-380

9. Sehitoglu, H., "Crack Opening and Crack Closure in Fatigue", Engineering Fracture Mechanics, V.21, No.2, 1985, pp.329-339

10. Blom,A.F, Holm,D.K " An Experimental and Numerical Study of Crack Closure", Engineering Fracture Mechanics, V.22, 1985, pp.997-1011

11. Nagtegaal J.C., Parks D.M and J.R.Rice, "On the Numerically Accurate Finite Element Solutions in the Fully Plastic Range", Comp. Methods Appl. Mech. Eng., V.4., 1974, pp.153-177